LEVEL # 0

(11) Jun 80

(12) 14

(6) A REACTION MECHANISM IN THE SHOCK INITIATION OF
DETONATION. A THEORETICAL STUDY, (U)

(10) *JACK ALSTER, NORMAN SLAGG, DR.
ARRADCOM, DOVER, NJ 07801   JUN 1980

MICHAEL J.S. DEWAR, JAMES P. RITCHIE, MR.
UNIVERSITY OF TEXAS, AUSTIN, TEXAS 78712

CHARLES WELLS, DR.
JUDSON COLLEGE, MARION, ALABAMA 36756

INTRODUCTION: In a chain explosion, the initial chemical reaction follows one or more modes of reaction (1,2). The ensuing highly reactive transient species, commonly believed to be radicals, react with intact explosive molecules to produce more radicals which ultimately recombine and release energy sufficient to support a detonation wave. To achieve better control over the detonation process it is important to know the rate of the relatively slow, primary reaction step and the nature of the transient species produced in this step. When, in particular, a condensed explosive experiences the high dynamic pressure of a strong, initiating shock wave, it may initiallly decompose via a bimolecular rather than a more commonly accepted unimolecular process. The present study was undertaken to examine this question in relation to the primary reaction step in liquid methyl nitrate undergoing shock initiation of detonation. In particular, the physical and chemical effects of the incident shock on the molecules are viewed in terms of the following three plausible modes of reaction:

1. Compression of a single molecule along its weakest bond, followed by scission of this bond as the molecule relaxes,

2. curling of fuel and oxidizer ends of the molecule towards each other followed by an intramolecular abstraction reaction, and

3. squeezing together of a pair of neighboring molecules such that the fuel end of one molecule reacts with the oxidizer end of the other.

91

80 10 15 038

393011

*Alster, Slagg, Dewar, Ritchie, & Wells

Methyl nitrate was chosen as the first of a series of explosives since the $H_3CO - NO_2$ bond is considerably weaker than the other bonds in the molecule. Hence, a theoretical treatment should yield more dramatic effects for this molecule than for a molecule which has a narrower distribution of bond energies. Moreover, methyl nitrate is a simple prototype of alkyl nitrate explosives such as nitroglycerine and pentaerythritol tetranitrate.

THEORETICAL PROCEDURES: The quantum chemical Modified Intermediate Neglect of Differential Overlap (MINDO/3) method (3) was employed. As a semi-empirical, self-consistent field molecular orbital treatment, it was parametrized by Dewar to yield equilibrium geometries and heats of formation for a wide variety of closed shell systems, including CHNO-molecules, giving good agreement with experiment (4). The parametrization apparently simulates the actual electric fields due to electrons and nuclei in stable, closed shell molecules. Thus, Dewar and coworkers predicted heats of formation with a mean absolute error of 5 kcal/mole. Equilibrium geometries are also satisfactory as bond lengths, bond angles and dihedral angles are given with mean absolute errors of .02Å , 6°, and 6° respectively. Although MINDO/3 was parametrized for just these equilibrium properties, it also predicts the activation energy for a variety of reactions involving complex organic molecules with a mean absolute error of 5 kcal/mole (5,6). It is, therefore, more than just a curve fitting technique as is also demonstrated by its ability to predict a variety of other molecular properties (5) that depend on the valence shell electron distribution.

MINDO/3 is used to calculate first the equilibrium geometry of the methyl nitrate molecule and then three minimum energy reaction paths (MERPs) (5,6) corresponding to the aforementioned three modes of reaction. Finally, values of the volume-, entropy-, and energy-of activation derived from the MERP are inserted into the absolute rate theory equation to yield the specific rate constant for a given reaction path at a given temperature and pressure. Of course, the most likely path to be followed under the given conditions will be the one with the highest rate constant.

GEOMETRY OF THE ISOLATED MOLECULE: Since the starting point for a chemical reaction is the equilibrium conformation of the molecule, its geometry is calculated first. A complete optimization of all bond distances, bond- and dihedral-angles was carried out. Figure 1 gives the overall shape of the molecule. The heavy atoms and one hydrogen atom H_1 are in the plane of the paper whereas the hydrogens H_a and H_b are above and below the plane, respectively. The staggered arrangement of the hydrogen atoms is correctly predicted.
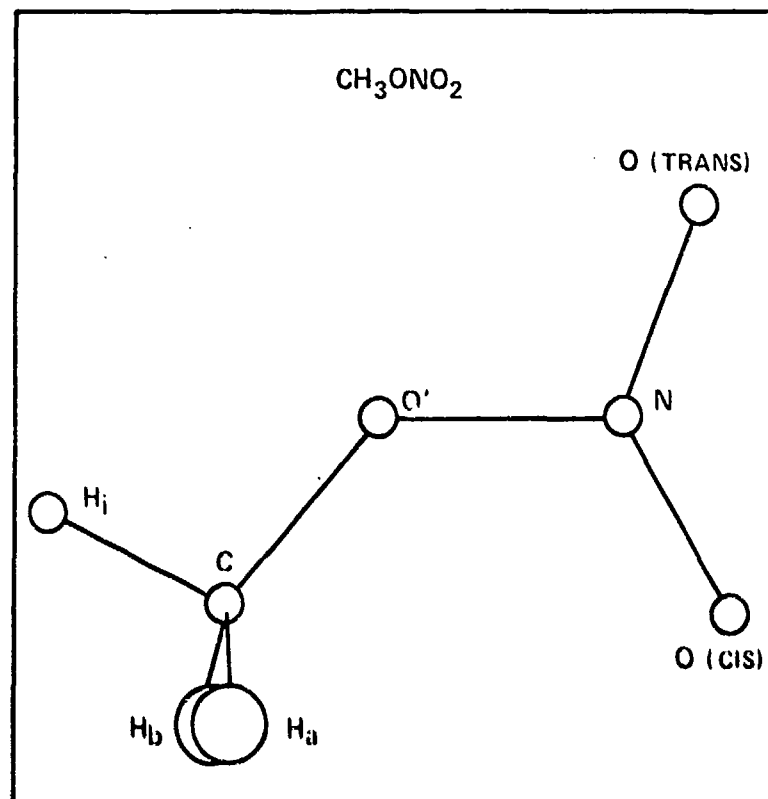
*Alster, Slagg, Dewar, Ritchie, & Wells

Figure 1. Calculated Shape of Methyl Nitrate Molecule

*Alster, Slagg, Dewar, Ritchie, & Wells

Moreover, calculated values for six bond distances and six bond angles agree with experimental values (obtained by microwave spectral measurements (7)) within mean absolute errors of 0.03Å and 5°, respectively. The heat of formation calculated for the equilibrium structure is -28.3 kcal/mole which also agrees well with the experimental value of -29.1 kcal/mole (8).

PROCEDURE FOR CALCULATING MERPS: In the course of generating the MERP beginning with the equilibrium geometry of the stable molecule, one encounters an uphill curve of total energy versus reaction variable. Here, we take for the variable either an interatomic distance or a bond angle. (For each chosen value of the reaction variable, the remaining molecular parameters are optimized to yield the lowest energy for that value of the reaction variable.) Eventually, a maximum is attained which, when compared to the initial energy, yields the activation energy for the assumed process.

The distorted molecular system corresponding to the energy maximum is known as the transition state or activated complex. Since the maximum is a saddle point, all energy gradients with respect to the molecular variables must vanish (9). This criterion is used to find the exact location of the transition state. Moreover, from the gradients at the extremum, second derivatives are calculated which represent the theoretical force constants. Since the transition state is stable to deformations along all coordinates other than the reaction coordinate, it has one and only one negative force constant. Thus, one can establish that the extremum corresponds to a transition state rather than a stable intermediate in which case all force constants are positive. In addition, a normal coordinate analysis is carried out on the transition state using the theoretical force constants as input. From the resulting set of normal modes of vibration, the vibration along the transition vector is selected for examination. In particular, it is determined whether the transition state indeed corresponds to the assumed reaction path and thus leads to the formation of the intended reaction products. Finally, after the transition state is located and characterized, all molecular parameters are optimized to yield final geometries and heats of formation of the reaction products.

UNIMOLECULAR REACTION PATHS

Scission of the Weakest Bond: Since $H_3CO - NO_2$ is the weakest bond in the molecule, a MERP corresponding to stretching this bond has been calculated. Table 1 gives heats of formation, H_f, of the equilibrium and transition states of the molecule and the activation energy, $\Delta E^{\ddagger}$, derived from the difference in H_f values.

94

Table 1. Properties of three plausible reaction paths of methyl nitrate

Species	Reaction type, R	H_f(kcal/mole)		$\Delta E^{\ddagger}$(kcal/mole)		ΔH_R(kcal/mole)	
		calc	obs.	calc	obs.	calc	obs.
Menitr*		-28.	-29.				
$[H_3CO - NO_2]^{\ddagger}$	Bond scission:	6.		34.	40	34.	40.
Menitr		-28.	-29.				
$\left[\begin{array}{c} H-O-N=O \\ H_2C-O \end{array} \right]^{\ddagger}$		28.					
H_2CO		-26.	-26.				
HONO	Intramol. H-Abstr:	-14.	-19.	56.		-11.	-16.
Menitr . Menitr		-57.					
$[\text{Menitr} \cdot \text{Menitr}]^{\ddagger}$		-24.					
CH_3ONO		-14.	-15.				
$(OH)H_2CO\ NO_2$	Bimol. O-Insert:	-73.	-71.**	33.		-31.	

* Menitr ≡ methyl nitrate

** Obtained via additivity rules.

123

The latter agrees reasonably well with the observed quantity. Figure 2 is a graphical representation of the MERP describing stretching of this bond to the point of scission. Finally, Figure 3 describes the geometry of the transition state and the transition vector, the arrows representing the amplitudes and directions of motion of the atoms in the normal coordinate corresponding to reaction. The methoxy oxygen-nitrogen bond $(O'-N)$ is stretched by $\sim 0.5Å$ from its original bond distance value of $1.4Å$ whereas all the other molecular parameters remain essentially unchanged.

Intramolecular Hydrogen Abstraction Reaction: The molecule is imagined to curl up, bringing a hydrogen atom into the vicinity of a terminal oxygen atom. The geometry of the transition state and the transition vector are depicted in Figure 4. The transition state is fully planar except for the non-ring hydrogens. Major changes in geometry which have occurred relative to the initial equilibrium conformation of Figure 1 are: $C-H_1$ and $O'-N$ bond distances have stretched by .25 and .2Å ,respectively, the O_{cis} - H distance has shrunk by $\sim 1.5Å$ and the $CO'N$ and $O'NO$ bond angles have collapsed by $\sim 27°$ and $10°$, respectively. The directions and magnitudes of the arrows in Figure 4 help visualize the manner in which planar H_2CO and trans-HONO are formed. The energetics of this reaction process are given in Table 1. The heats of formation of reactant and product molecules and the resulting exothermic heat of reaction ΔH_R are predicted with reasonable accuracy. Moreover, $\Delta E^{\ddagger}$ is ~ 20 kcal/mole higher than that of the unimolecular bond scission process.

BIMOLECULAR REACTION PATH: In this reaction path two molecules of methyl nitrate are brought together in such a way that the methyl group of one molecule interacts with the nitrate group of the other, as shown in Figure 5. In fact, the figure represents the transition state in which reaction is imminent. The arrows on the atoms in the reaction site suggest insertion of an oxygen atom into the $C-H_1$ bond in the plane of the heavy atoms. Thus, methyl nitrite and hydroxmethyl nitrate are predicted as products. Although the latter molecule is not known, it appears to have some thermodynamic stability as is illustrated by its very negative heat of formation. According to Table 1, the reaction requires an activation energy of 32 kcal/mole which is comparable to that of the unimolecular bond scission process. Moreover, the reaction is exothermic by ~ 31 kcal/mole. Hence, the molecules could act as energy carriers in a reaction sequence leading to detonation.

CALCULATION OF REACTION RATES: Assuming that thermal equilibrium exists between the transition state and the stable

96

(24)

*Alster, Slagg, Dewar, Ritchie, & Wells
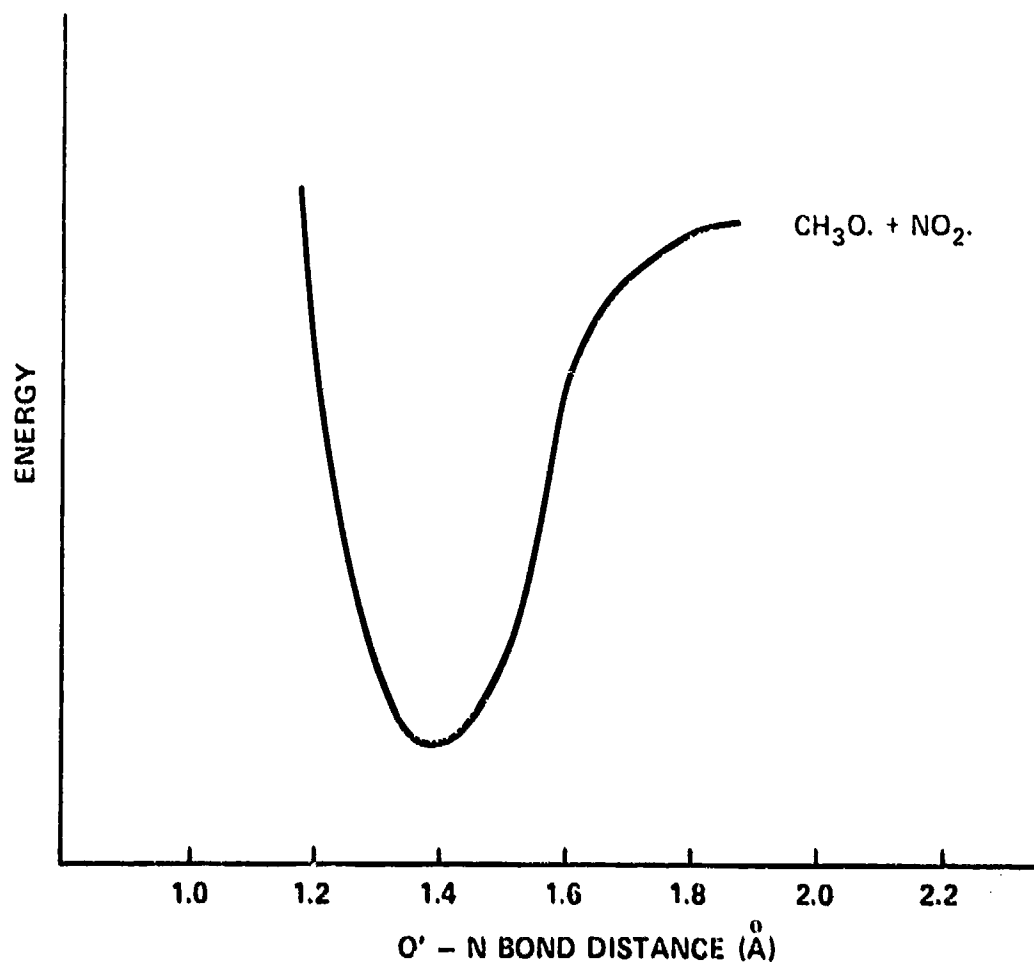

Figure 2.   MERP of the Bond Scission Reaction in Methyl Nitrate

*Alster, Slagg, Dewar, Ritchie, & Wells
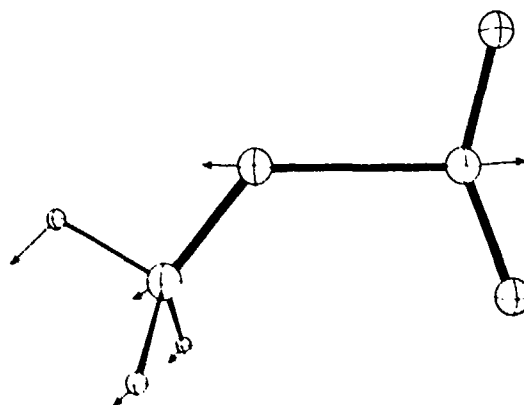

Figure 3.   Shape and Transition Vector of the Bond Scission Transition
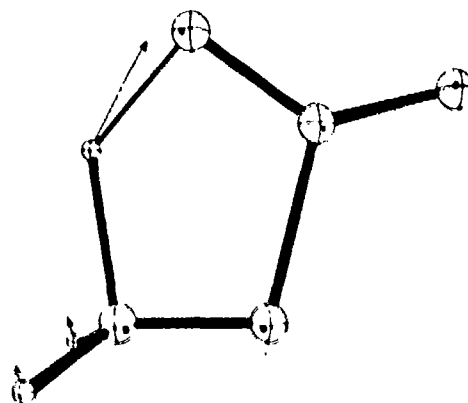State of Methyl Nitrate

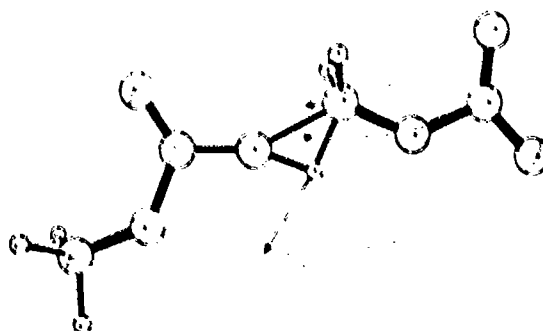Figure 4.   Shape and Transition Vector of the Cyclic Transition State
of Methyl Nitrate

Figure 5.   Shape and Transition Vector of the Bimolecular Transition State
of Methyl Nitrate

98

molecule, the specific reaction rate constant is given by the following thermodynamic formulation of transition state theory:

$$k = \frac{KT}{h} \cdot \exp\left(\frac{-P\Delta V^{\ddagger}}{RT}\right) \cdot \exp\left(\frac{\Delta S^{\ddagger}}{R}\right) \cdot \exp\left(\frac{-\Delta E^{\ddagger}}{RT}\right) \quad (1)$$

where $\Delta S^{\ddagger}$, $\Delta V^{\ddagger}$, and $\Delta E^{\ddagger}$ are entropies-, volumes-, and energies-of-activation, respectively. In order to assess the relative importance of different reaction paths, we must evaluate or, at least, estimate these quantities for each path. The MERPs have been analyzed, in fact, to provide values for these quantities. In particular, $\Delta V^{\ddagger}$ and the rotational contribution to $\Delta S^{\ddagger}$ are obtained from the calculated geometries of the stable methyl nitrate molecule and the different transition states. Moreover, the vibrational contribution to $\Delta S^{\ddagger}$ is derived from the vibrational frequencies generated by a normal coordinate analysis. Finally, $\Delta S^{\ddagger}$ is obtained as the sum of these contributions and that of translation, the latter being readily calculated from the molecular weights of the reactant and transition state species (10). This procedure gives good agreement between calculated values of the volume and entropy of the stable methyl nitrate molecule at 298K and 1 atm viz. $115Å^3$ and 74.5 eu, respectively and the corresponding values derived from experiment viz. $106Å^3$ and 75.9 eu (11,12).

Since Equation 1 interrelates a vast body of chemical kinetic information on reactions in both gas- and condensed-phases (13), we apply it to the case at hand which is shock initiation of liquid methyl nitrate. Low-and high- velocity detonations have been measured in liquid methyl nitrate (14). However, the pressure and temperature conditions associated with the initiating shock were not determined. We, therefore, estimated a typical set of values for liquid methyl nitrate based on (1) a measurement by Campbell et al. (15) of the pressure and associated temperature of an initiating shock wave in liquid nitromethane and (2) measurements by Shaw (16) on pressures and corresponding reaction times for initiating shocks in nitromethane and methyl nitrite liquids. The values thus estimated for liquid methyl nitrate are 60 kbars and 800K.

To make proper use of Equation 1, values of the activation parameters $\Delta V^{\ddagger}$, $\Delta S^{\ddagger}$, and $\Delta E^{\ddagger}$ should correspond to the elevated temperature and pressure associated with the initiating shock wave. Therefore, $\Delta S^{\ddagger}$ and $\Delta E^{\ddagger}$ were calculated for 800K via the use of statistical thermodynamic relations involving partition functions but $\Delta V^{\ddagger}$ which had been calculated for 298K is assumed to be constant over the temperature range 298-800K. As for the pressure dependence

99

of these properties experimental evidence in the literature (17,18) indicates that for several unimolecular and bimolecular reactions carried out in the pressure range .001-60 kbars, their combined effect on specific rate constants is no greater than two orders of magnitude. As shown in Table 2, the rate constants at 60 kbars and 800K differ by many more orders of magnitude. Clearly, the first exponential term in Equation 1 overshadows the pressure dependence of the activation parameters.

DISCUSSION OF RESULTS

Table 2 shows that at 60 kbars and 800K the specific rate constant for bond scission is four orders of magnitude larger than that of the intramolecular hydrogen abstraction reaction. Of greater interest is the finding that the specific rate constant for the bimolecular reaction is nine orders of magnitude greater than the faster of the two unimolecular reaction processes. It is apparent from Table 2, that this is entirely due to the highly compressed form of the bimolecular transition state, viz. $\Delta V^{\ddagger} = -32.2$ cc/mole. This, in turn, results from the formation of C-O and O-H bonds at the expense of rupture of an N-O bond during the oxygen insertion reaction. This is, in fact, the first time that theory suggests a reaction in which a bound $-NO_2$ group directly donates its oxygen to another molecule. Traditionally, it has been assumed that oxidation occurs only after the formation of the NO_2 molecule. Since MINDO/3 was originally parametrized for equilibrium properties and its reliability for predicting activation parameters of insertion reactions has not yet been established, it is planned to put these conclusions to an experimental test.

Nevertheless, the results are consistent with thermo-hydrodynamic predictions and observed detonation phenomena. In particular, a finding from Figure 6 that the bimolecular methyl nitrate system compresses by ~ 23% on reaching the transition state accords with thermo-hydrodynamic predictions of a maximum compression of condensed explosives by strong shock waves of 25-37.5% (15,19). Similarly, a 5% compression of a single methyl nitrate molecule along the repulsive portion of the curve in Figure 2 to a state isoenergetic with the transition state for bond scission is also consistent with thermohydrodynamics. It is clear that most of the compression by shock is due to intermolecular rather than intramolecular processes. With respect to detonation phenomena, Kusakabe and Fujiwara (14) observed that liquid methyl nitrate propagates at a stable, low velocity detonation (LVD) of ~ 2500 m/s when the initiating shock pressure is low and high velocity detonation (HVD) of ~ 6700 m/s when
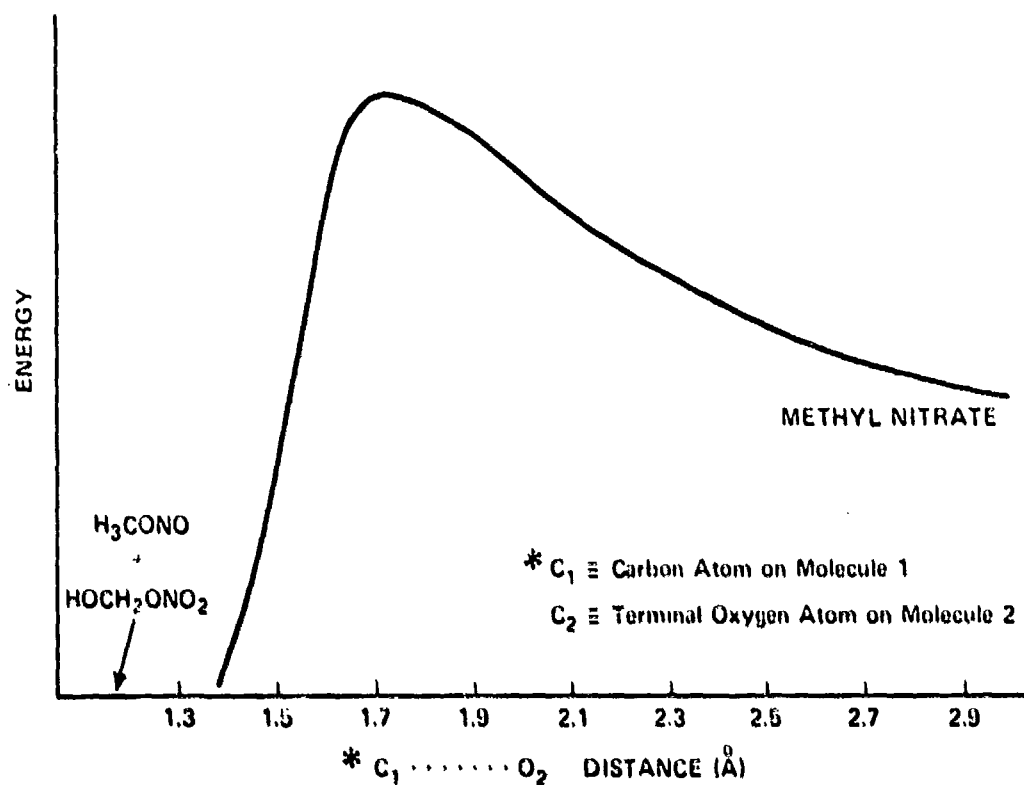
Figure 6. MERP of the Bimolecular Reaction in Methyl Nitrate

Table 2. Transition State Parameters and Relative Rates of
Reaction, $k_x/k_{bond\ sciss.}$ at 800K and 60 kbars.

	$\Delta V^{\ddagger}$ (cc/mole)	$\Delta S^{\ddagger}$ (cal/mole-deg)	$\Delta E^{\ddagger}$ (kcal/mole)	$k_x k_{bond\ sciss}$
Bond Scission:	5.4	-1.4	34.0	1.0
Intramolecular H-Abstraction:	-2.1	-4.2	56.5	10^{-4}
Bimolecular O-Insertion:	-32.2	-32.3	32.3	10^{9}

*Alster, Slagg, Dewar, Ritchie, & Wells

the pressure is high. In view of the importance of the exp $(-P\Delta V^{\ddagger}/RT)$ term in the rate expression, our calculations show that the HVD phenomenon is explainable in terms of the fast bimolecular process and LVD in terms of the much slower unimolecular bond scission process. The exothermicity of the bimolecular reaction path as opposed to the endothermicity of the unimolecular bond scisson path provides yet another reason for relating these processes with HVD and LVD, respectively. Thus, energy to support the HVD front could become available to it immediately from the bimolecular reaction step whereas energy for the LVD front would be forthcoming from radical recombination reaction steps which occur much later and many reaction steps after the primary bond scission step (2).

SUMMARY AND CONCLUSIONS

A theoretical approach is described which permits one to calculate rates of reaction from the structural formula of an explosive molecule. The theoretical tools are the MINDO/3 semi-empirical quantum chemical procedure of Dewar and the transition theory rate equation. The applicability of this approach to the study of shock initiation of detonation is illustrated by way of the liquid explosive, methyl nitrate. The relative rates of three plausible reaction paths are calculated. They are the unimolecular bond scission reaction which yields $CH_3O\cdot$ and $NO_2\cdot$, the intramolecular hydrogen abstraction reaction which yields HONO and H_2CO and the bimolecular oxygen insertion reaction which yields CH_3ONO and $HOCH_2ONO_2$. Surprisingly, it was found that at conditions believed to be typical for shock initiation of high velocity detonation in liquid methyl nitrate viz. 60 kbars and 800K, the bimolecular reaction proceeds nine orders of magnitude faster than the commonly accepted bond scisson reaction whereas the intramolecular reaction is four orders of magnitude slower than bond scission. Moreover, the bimolecular reaction is exothermic by ~ 30 kcal/mole. If experimentally confirmed, this finding would represent the first instance of a reaction in which a bound NO_2 group directly inserts oxygen into the bond of another molecule. The results are consistent with thermohydrodynamic predictions for shock compression of condensed explosives and with observations of stable high velocity and low velocity detonation in liquid methyl nitrate.

The approach taken here has yielded a new view of processes in the detonation regime. It is recognized that future experimental observations are needed to confirm the above conclusions. Moreover, it is felt that, in addition to the use of a semi-empirical quantum chemical procedure, a combination of a state-of-the-art ab initio

*Alster, Slagg, Dewar, Ritchie, & Wells

method and new experimental techniques for monitoring transient chemical species can provide new insights into detonation phenomena.

REFERENCES

1. N.N. Semenov, "Some Problems of Chemical Kinetics and Reactivity", Volume 1, translated by J.E.S. Bradley, Pergamon Press, NY, NY, 1958.

2. J. Alster, and N. Slagg, "Proceedings of the Conference on Mechanisms of Explosions and Blast Waves, sponsored by JTCG/ALNNO, US ARRADCOM, Dover, NJ (November 1973) p. XV.

3. R.C. Bingham, M.J.S. Dewar, and D.H. Lo, J. Am. Chem. Soc. 97, 1285 (1975).

4. Ibid, 1302.

5. M.J.S. Dewar, Science, 187, 1037 (1975).

6. M.J.S. Dewar, Faraday Discussions of the Chem. Soc. 62, 197 (1977).

7. A.P. Cox and S. Waring, Trans. Faraday Soc. 76 , 3441 (1971).

8. J.D. Cox and G. Pilcher, "Thermochemistry of Organic and Organometallic Compounds," Academic Press, NY, NY, 1970.

9. J.W. McIver and A. Komornicki, Chem. Phys. Lett. 10, 303 (1971).

10. G. Herzberg, "Molecular Spectra and Molecular Structure, II. Infrared and Raman Spectra of Polyatomic Molecules," Chapter V, D. Van Nostrand Co., Inc., NY, NY, 1945.

11. J.A. Dean, Lange's Handbook of Chemistry, 11th Edition, McGraw Hill Book Co., NY, NY, 1973.

12. J.C.D. Brand and T.M. Cawthon, J. Am. Chem. Soc. 77, 319 (1955).

13. I. Amdur and G.G. Hammes, "Chemical Kinetics, Principles and Selected Topics," McGraw-Hill Book Co., NY, NY, 1966, p. 44.

14. M. Kusakabe and S. Fujiwara, Fifth Symposium of Detonation, sponsored by US Naval Surface Weapons Center, White Oak, MD and Office of Naval Research, Washington, DC (1970).

(131)

*Alster, Slagg, Dewar, Ritchie, & Wells

15. A.W. Campbell, W.C. Davis, and J.R. Travis, Physics of Fluids 4, 498 (1961).

16. R. Shaw, Combustion and Flame 21 127 (1973).

17. R.S. Bradley, "High Pressure Physics and Chemistry," Volume 2, Chapter 8, "Chemical Kinetics" by S.D. Hamman, Academic Press, NY, NY, 1963.

18. R.S. Bradley, Ibid, Chapter 9, Table II, p. 227.

19. J. Taylor, "Detonation in Condensed Explosives," Oxford University Press, London, 1952.